ISSN 1070-3284, Russian Journal of Coordination Chemistry, 2019, Vol. 45, No. 6, pp. 467–471. © Pleiades Publishing, Ltd., 2019.

Synthesis and Crystal Structure of a Dioxomolybdenum(VI) Complex Derived from 2-Bromo-*N'*-(3,5-Dichloro-2-Hydroxybenzylidene)benzohydrazide with Catalytic Epoxidation Property

Y. Q. Zhou[a, b], W. T. Liu[c], R. D. Lu[a], Y. B. Jin[a], M. D. Yang[a], Wu Chen[a], and Y. M. Cui[a, d, *]

[a]*National Local Joint Enginering Laboratory for Advanced Textile Processing and Clean Production, Wuhan Textile University, Wuhan, 430073 P.R. China*

[b]*School of Chemistry, Huazhong Normal University, Wuhan, 430079 P.R. China*

[c]*China Meheco Liyi Pharm Sci and Tech Co., Ltd., Wuhan, 430073 P.R. China*

[d]*School of Environmental Engineering, Wuhan Textile University, Wuhan, 430073 P.R. China*

**e-mail: cuiym981248@163.com*

Received May 21, 2018; revised June 6, 2018; accepted October 18, 2018

Abstract—A dioxomolybdenum(VI) complex [$MoO_2L(EtOH)$] (**I**), derived from the hydrazone ligand 2-bromo-*N'*-(3,5-dichloro-2-hydroxybenzylidene)benzohydrazide has been prepared and characterized by physico-chemical and spectroscopic methods, as well as single crystal X-ray diffraction (CIF file CCDC no. 1840671). The hydrazone ligand coordinates to the Mo atom through the phenolate oxygen, imino nitrogen, and enolic oxygen. The Mo atom is six-coordinate in an octahedral geometry. Complex **I** shows high catalytic activity and selectivity in the epoxidation of cyclohexene with *tert*-butylhydroperoxide as primary oxidant.

Keywords: hydrazone, dioxomolybdenum(VI) complex, crystal structure, catalytic property

DOI: 10.1134/S1070328419060101

INTRODUCTION

Molybdenum complexes have attracted remarkable attention due to their effective catalytic properties for a variety of organic reactions [1–3], particularly for sulfoxidation and epoxidation of olefins [4–6]. Hydrazone compounds play an important role in coordination chemistry. Molybdenum complexes derived from hydrazones have been reported to possess effective catalytic properties [7–9]. However, the number of such complexes is scarce. Recently, we have reported some complexes with hydrazone ligands [10, 11]. In continuation of these studies, in the present work, a dioxomolybdenum(VI) complex [$MoO_2L(EtOH)$] (**I**), where H_2L is 2-chloro-*N'*-(hydroxy-5-methoxybenzylidene)benzohydrazide (Scheme 1), is reported.

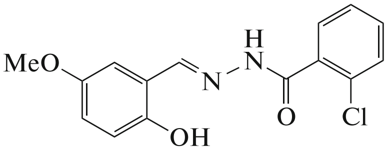

Scheme 1.

EXPERIMENTAL

Materials and methods. 5-Methoxysalicylaldehyde and 2-chlorobenzohydrazide were purchased from Alfa Aesar. [$MoO_2(Acac)_2$] was prepared according to the literature method [12]. All chemicals and solvents were of analytical grade and used as obtained. Microanalyses for C, H, and N were obtained with a Vario EL III CHNOS elemental analyzer. Infrared spectra were recorded as KBr pellets with an FTS-40 spectrophotometer. UV-Vis spectra were recorded on a Lambda 900 spectrometer. ^1H NMR data were recorded on a Bruker 500 MHz spectrometer.

Synthesis of H_2L. 5-Methoxysalicylaldehyde (0.01 mol, 1.52 g) and 2-chlorobenzohydrazide (0.01 mol, 1.71 g) were dissolved in ethanol (50 mL). The mixture was stirred at reflux for 30 min to give a colorless solution. The solvent was evaporated and the solid was recrystallized from ethanol to give crystalline product of H_2L. The yield was 0.28 g (92%). IR (KBr; ν_{max}, cm^{-1}): 3413 w (OH), 3175 w (NH), 1643 s (C=O), 1598 s (C=N), 1172 w (C–O, phenolate), 1035 w (N–N). UV-Vis data in acetonitrile (λ_{max}, nm, ε (L mol^{-1} cm^{-1})): 295 (18720), 302 (17155), 353 (7545). ^{1}H NMR (500 MHz; DMSO; δ, ppm): 12.13 (s., 1H, OH), 10.57 (s., 1H, NH), 8.81 (s., 1H, CH=N), 7.71–7.62 (m., 2H, ArH), 7.53 (t., 1H, ArH), 7.37 (d., 1H, ArH), 7.28 (s., 1H, ArH), 6.93–6.85 (q., 2H, ArH), 3.77 (s., 3H, OCH_3).

For $C_{15}H_{13}N_2O_3Cl$

Anal. calcd., %	C, 59.1	H, 4.3	N, 9.2
Found, %	C, 58.9	H, 4.4	N, 9.1

Synthesis of complex (I). H_2L (1.0 mmol, 0.305 g) in ethanol (20 mL) was mixed with $[MoO_2(Acac)_2]$ (1.0 mmol, 0.326 g), and the resulting reaction mixture was boiled under reflux for 1 h, then cooled to room temperature, yielding a yellowish solution. The solution was left to evaporate at ambient temperature for a week, yielding orange block-shaped single crystals of the complex. The yield was 0.27 g (57%).

IR (KBr; ν_{max}, cm^{-1}): 3377 w (OH), 1605 s (C=N), 1350 m (C–O, enolic), 1155 w (C–O, phenolate), 1059 s (N–N), 948 m and 892 s (Mo=O). UV-Vis data in acetonitrile (λ_{max}, nm, ε (L mol^{-1} cm^{-1})): 287 (16550), 327 (7860), 400 (1730). ^{1}H NMR (500 MHz; DMSO; δ, ppm): 8.98 (s., 1H, CH=N), 7.87 (d., 1H, ArH), 7.65 (d., 1H, ArH), 7.45–7.30 (m., 3H, ArH), 6.93–6.82 (q., 2H, ArH), 3.77 (s., 3H, OCH_3), 3.45 (q., CH_3CH_2OH), 1.13 (t., CH_3CH_2OH).

For $C_{17}H_{17}N_2O_6ClMo$

Anal. calcd., %	C, 42.8	H, 3.6	N, 5.9
Found, %	C, 43.0	H, 3.7	N, 5.8

X-ray structural determination. Data were collected on a Bruker SMART 1000 CCD area diffractometer using graphite-monochromated MoK_α radiation (λ = 0.71073 Å) at 298(2) K, and corrected with the SADABS program [13]. The structure was solved by direct methods [14] and refined on F^2 by full-matrix least-squares using the SHELXL program [15]. All non-hydrogen atoms were refined anisotropically. The ethanol hydrogen atom was located from a difference Fourier map and refined isotropically with O–H distance restrained to 0.85(1) Å. The remaining hydrogen atoms were placed in calculated positions as riding model. Crystal data and details of the data collection and refinement are listed in Table 1. Selected bond lengths and angles are listed in Table 2.

Supplementary material for structure **I** has been deposited with the Cambridge Crystallographic Data Centre (CCDC no. 1840671; deposit@ccdc.cam.ac.uk or http://www.ccdc.cam.ac.uk).

Catalytic epoxidation tests. Epoxidation of cyclohexene by the dioxomolybdenum(VI) complex with *tert*-butyl hydroperoxide (TBHP) was carried out according to the following procedure. A mixture of catalyst (0.003 mmol), cyclohexene (6.56 g, 0.08 mol) and 1,2-dichloroethane (5 mL) was placed in a three-necked round-bottomed flask equipped with a condenser and a magnetic stirrer. The mixture was stirred for 5 min at 353(2) K and then anhydrous TBHP (2 mL, 0.2 mol) was added. The reaction was monitored at certain time intervals to determine the concentrations of TBHP and 1,2-epoxycyclohexane by GC and was allowed to proceed until near complete conversion of TBHP.

RESULTS AND DISCUSSION

$[MoO_2(acac)_2]$ reacted with H_2L in ethanol gave the dioxomolybdenum(VI) complex. The hydrazone ligand adopts enolic tautomeric form. The yellow single crystals of the complex are stable in air at ambient condition.

The weak and broad bands centered at 3413 and 3377 cm^{-1} in the spectra of H_2L and **I**, respectively, are assigned to the ν(O–H) vibrations. The weak band at 3175 cm^{-1} in the spectrum of H_2L is assigned to the ν(N–H) vibration. The strong band at 1643 cm^{-1} of the free hydrazone is assigned to ν(C=O) vibration. The ν(C=O) and ν(NH) vibrations are absent in the spectrum of **I**, indicating enolization of the amide functionality with concomitant substitution of the proton by the molybdenum atom, which is in accordance with the results obtained by X-ray crystallography. The ν(C–O)(enolic) mode of the complex is observed at 1350 cm^{-1}, which is absent in the spectrum of the free hydrazone. The strong bands at 1598 cm^{-1} for H_2L and 1605 cm^{-1} for **I** are assigned to the azomethine groups [16]. The typical bands observed at 948 and 892 cm^{-1} for the complex are assigned to the Mo=O stretches [17].

The UV-Vis spectrum of I displays both strong and medium absorption bands centered at 400 and 327 nm. These peaks are assigned to charge transfer transitions of the type N($p\pi$)–Mo($d\pi$) LMCT and O($p\pi$)–Mo($d\pi$) LMCT, respectively [18], since the ligand-based orbitals are either N or O donor types. The intense bands centered at 295 nm for H_2L and 287 nm for **I** can be assigned to $\pi\rightarrow\pi^*$ transitions.

Figure 1 gives perspective view of the complex, together with the atomic labeling system. The hydrazone ligand forms five- and six-membered chelate rings with bite angles of 71.0(2)° and 81.4(2)°. The Mo atom occupies a distorted octahedral O_5N coordination sphere. The phenolate oxygen, imino nitrogen, and enolic oxygen of the hydrazone ligand, together with one oxo oxygen constitute the equatorial plane, with the maximum deviation of the atoms constituting the mean plane of 0.0266 Å. The axial positions are occupied by one oxo oxygen and one ethanol oxygen. The displacement of the Mo atom from the equatorial plane towards the axial oxo group is 0.319(1) Å. The *cis* and *trans* bond angles are in the ranges of 71.0(2)°–

Table 1. Crystallographic data and structure refinements for complex **I**

Parameters	Value
Mr	476.72
T, K	298(2)
Crystal shape/color	Block/yellow
Crystal size, mm	0.30 × 0.27 × 0.23
Crystal system	Triclinic
Space group	$P\bar{1}$
a, Å	8.253(2)
b, Å	10.593(2)
c, Å	10.789(2)
α, deg	77.473(2)
β, deg	89.764(2)
γ, deg	85.366(2)
V, Å^3	917.7(3)
Z	2
ρ_{calcd}, g cm^{-3}	1.725
$\mu(MoK_\alpha)$, cm^{-1}	0.898
F(000)	480
Reflections collected	5453
Unique reflections (R_{int})	3395 (0.0460)
Observed reflections $I \geq 2\sigma(I)$	2338
Min and max transmission	0.7745 and 0.8202
Refinement parameters	249
Restraints	1
Goodness-of-fit on F^2	1.033
R_1, wR_2 ($I \geq 2\sigma(I)$)*	0.0542, 0.1193
R_1, wR_2 (all data)*	0.0890, 0.1529
Large diff. peak and hole, e Å^{-3}	0.628/–0.834

* $R_1 = \Sigma||F_o|-|F_c||/\Sigma|F_o|$, $wR_2 = [\Sigma w(F_o^2 - F_c^2)^2/\Sigma w(F_o^2)^2]^{1/2}$.

Table 2. Selected bond lengths (Å) and angles (deg) for complex **I**

Bond	*d*, Å	Bond	*d*, Å
Mo(1)–O(1)	1.907(4)	Mo(1)–O(2)	2.018(4)
Mo(1)–O(3)	1.674(5)	Mo(1)–O(4)	1.694(5)
Mo(1)–O(5)	2.387(5)	Mo(1)–N(1)	2.237(5)
Angle	**ω, deg**	**Angle**	**ω, deg**
O(3)Mo(1)O(4)	105.9(2)	O(3)Mo(1)O(1)	99.0(2)
O(4)Mo(1)O(1)	102.3(2)	O(3)Mo(1)O(2)	96.2(2)
O(4)Mo(1)O(2)	98.9(2)	O(1)Mo(1)O(2)	149.34(19)
O(3)Mo(1)N(1)	94.7(2)	O(4)Mo(1)N(1)	158.2(2)
O(1)Mo(1)N(1)	81.39(18)	O(2)Mo(1)N(1)	70.97(17)
O(3)Mo(1)O(5)	169.7(2)	O(4)Mo(1)O(5)	83.5(2)
O(1)Mo(1)O(5)	82.7(2)	O(2)Mo(1)O(5)	77.84(19)
N(1)Mo(1)O(5)	75.54(18)		

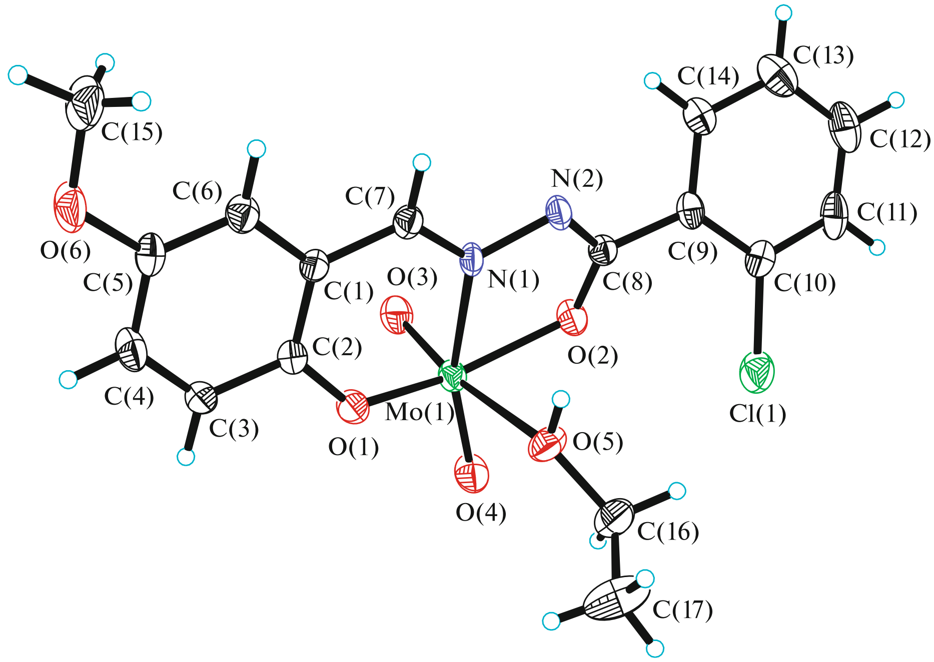

Fig. 1. ORTEP plots (30% probability level) and atom labeling scheme for complex **I**.

105.9(2)° and 149.3(2)°–169.7(2)°, respectively. The Mo–O and Mo–N bond lengths in **I** are comparable to those reported for other dioxomolybdenum(VI) complexes with hydrazone ligands [19–21]. As commonly observed in analogous complexes, the elongated Mo(1)–O(5) bond *trans* to the oxo group (O(3)) indicates weak coordination of the ethanol ligand at the axial position. The dihedral angle between the two benzene rings in **I** is 18.6(5)°. The relatively large deviations from linearity in the O(1)Mo(1)O(2) angle of 149.3(2)° can be attributed to the strain created by the five- and six-membered chelate rings. The distance between atoms C(8) and N(2) (1.307(8) Å) is shorter than normal N=C bonds, whilst the distance between atoms C(8) and O(2) (1.294(7) Å) is longer than normal O=C bonds, indicating enolisation of the N(2)–C(8)–O(2) group.

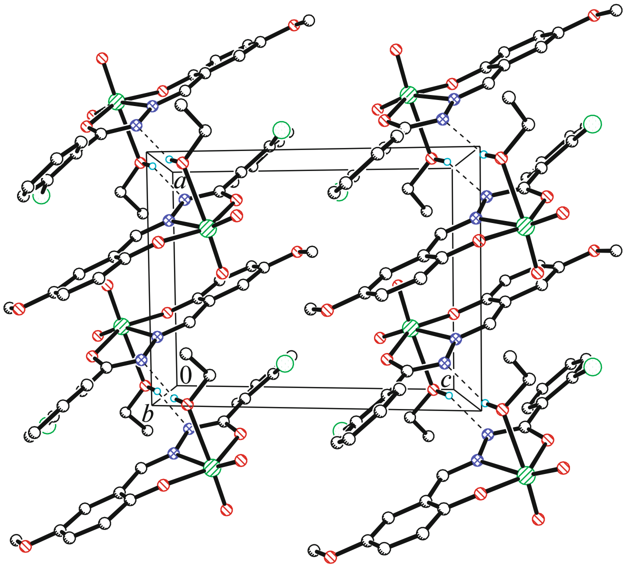

Fig. 2. Molecular packing structure of the complex. Hydrogen bonds are shown as dashed lines.

In the crystal structure of **I**, adjacent pairs of molecules are linked via intermolecular O–H···N hydrogen bonds (O(5)–H(5) 0.85(1) Å, H(5)···N(2)^{i} 2.16(4), O(5)···N(2)^{i} 2.944(7) Å, O(5)–H(5)···N(2)^{i} 154(8)°; ^{i} $2 - x, 1 - y, -z$), forming a dimer (Fig. 2).

The catalytic property of **I** was determined by the yields for epoxidation of cyclohexene using TBHP as oxidant. The yields were calculated as $Y = (c_{\mathrm{epox}}/c_{\mathrm{TBHP}}) \times 100\%$, where c_{epox} and c_{TBHP} (mol L^{-1}) are the concentration of epoxide formed and the initial concentration of TBHP, respectively. The selectivity with respect to the TBHP was calculated by the ratio $S = (c_{\mathrm{epox}}/(c_{\mathrm{TBHP}} - c)) \times 100$, where c is the final TBHP concentration. The yields are shown in Fig. 3. After 25 min of reaction, the yields were nearly quantitative with selectivity of 100%. The catalytic oxidation property of **I** is in accordance with these of similar dioxomolybdenum(VI) complexes reported in the literature [5, 22].

According to Sobczak's proposal [23], the probable mechanism of the catalytic epoxidation is shown in Scheme 2. First, formation of the intermediate complex [MoO$_2$L(*t*-BuOOH)] gives rise to activation of TBHP. Second, interaction between the cyclohexene and TBHP molecule is promoted by the molybdenum

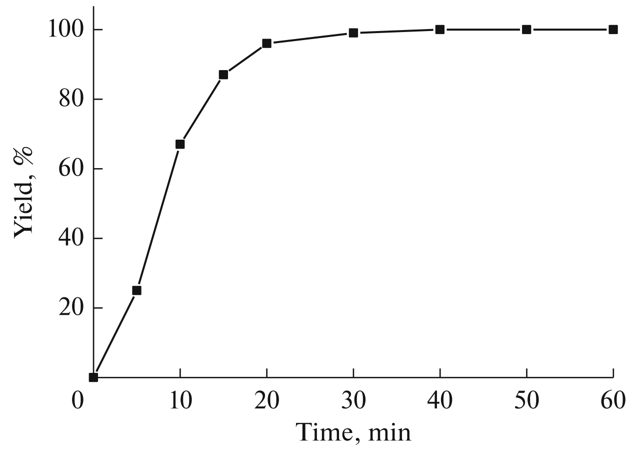

Fig. 3. Yield and time curve of the catalytic epoxidation reaction.

complex. Third, the epoxide is formed, converting TBHP into *t*-BuOH. Finally, substitution of *t*-BuOH by TBHP regenerates the intermediate complex [MoO_2L(*t*-BuOOH)].

Proposed mechanism of cyclohexene epoxidation with complex **I** and TBHP as primary oxidant are given below:

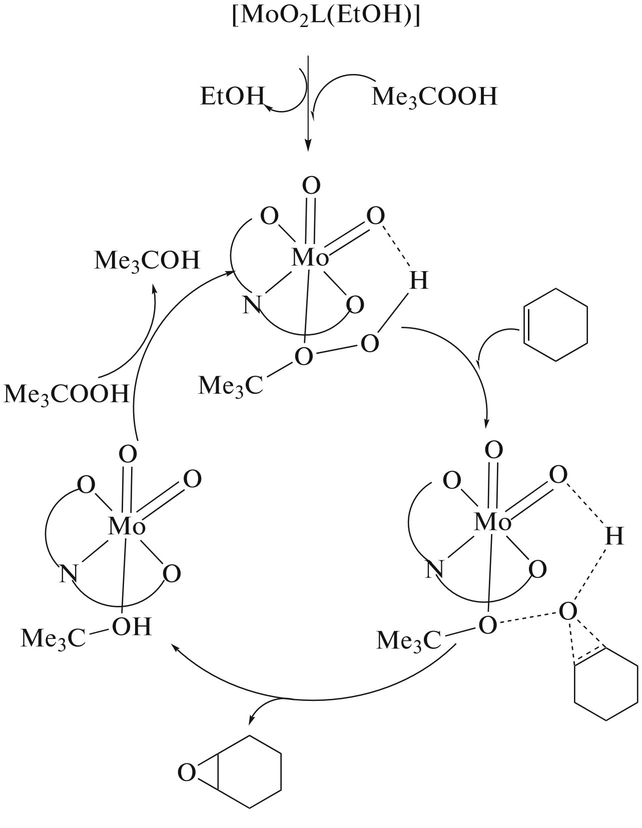

Scheme 2.

A dioxomolybdenum(VI) complex was prepared and structurally characterized by single crystal X-ray determination. The dianionic hydrazone acts as a tridentate ligand, through the phenolate oxygen, imino nitrogen and enolic oxygen. The complex shows promise as catalyst for the epoxidation of cyclohexene. Further work on the catalytic application of complex **I** is under way in our laboratory.

REFERENCES

1. Gamelas, C.A., Gomes, A.C., Bruno, S.M., et al., *Dalton Trans.*, 2012, vol. 41, no. 12, p. 3474.
2. Reithofer, M.R., Schrock, R.R., and Muller, P., *J. Am. Chem. Soc.*, 2010, vol. 132, no. 24, p. 8349.
3. Wong, Y.-L., Tong, L.H., Dilworth, J.R., et al., *Dalton Trans.*, 2010, vol. 39, no. 19, p. 4602.
4. Rayati, S., Rafiee, N., and Wojtczak, A., *Inorg. Chim. Acta*, 2012, vol. 386, p. 27.
5. Amarante, T.R., Neves, P., Tome, C., et al., *Inorg. Chem.*, 2012, vol. 51, no. 6, p. 3666.
6. Bagherzadeh, M., Amini, M., Ellern, A., et al., *Inorg. Chem. Commun.*, 2012, vol. 15, p. 52.
7. Rao, S.N., Munshi, K.N., Rao, N.N., et al., *Polyhedron*, 1999, vol. 14, nos. 17–18, p. 2491.
8. Bagherzadeh, M., Amini, M., Parastar, H., et al., *Inorg. Chem. Commun.*, 2012, vol. 20, p. 86.
9. Sui, Y., Zeng, X., Fang, X., et al., *J. Mol. Cat., A*, 2007, vol. 270, nos. 1–2, p. 61.
10. Cui, Y.-M., Cai, Y.-J., and Chen, W., *J. Coord. Chem.*, 2011, vol. 64, no. 8, p. 1385.
11. Cui, Y.-M., Cai, Y.-J., and Chen, W., *Russ. J. Coord. Chem.*, 2011, vol. 37, no. 12, p. 908. https://doi.org/10.1134/S1070328411110017
12. Chen, G.J.J., McDonald, J.W., and Newton, W.E., *Inorg. Chem.*, 1976, vol. 15, no. 11, p. 2612.
13. Sheldrick, G.M., *SADABS, Siemens Analytical X-ray Instrument Division*, Madison). 1995.
14. Sheldrick, G.M., *Acta Crystallogr., Sction A: Found. Crystallogr.*, 2008, vol. 64, no. 1, p. 112.
15. Sheldrick, G.M., *SHELXTL, Version 5.1*, Bruker Analytical X-ray Instruments Inc., Madison, 1998.
16. Ngan, N.K., Lo, K.M., and Wong, C.S.R., *Polyhedron*, 2011, vol. 30, no. 17, p. 2922.
17. Glowiak, T., Jerzykiewicz, L., Sobczak, J.M., et al., *Inorg. Chim. Acta*, 2003, vol. 356, p. 387.
18. Gupta, S., Barik, A.K., Pal, S., et al., *Polyhedron*, 2007, vol. 26, no. 1, p. 133.
19. Takjoo, R., Ramasami, P., Mague, J.T., et al., *J. Coord. Chem.*, 2016, vol. 69, no. 6, p. 1100.
20. Amini, M., Khaksar, M., Boghaei, D.M., et al., *J. Coord. Chem.*, 2014, vol. 67, no. 14, p. 2435.
21. Pasayat, S., Dash, S.P., Majhi, P.K., et al., *Polyhedron*, 2012, vol. 38, no. 1, p. 198.
22. Moradi-Shoelili, Z., Zare, M., Bagherzadeh, M., et al., *J. Coord. Chem.*, 2015, vol. 68, no. 3, p. 548.
23. Sobczak, J. and Ziolkowski, J.J., *J. Mol. Catal.*, 1981, vol. 13, no. 1, p. 11.